Journal of Ceramic Processing Research. Vol. 18, No. 1, pp. 21~26 (2017)

J O U R N A L O F
Ceramic Processing Research

Preparation and mechanical properties of alumina/spinel/metal composite with three different sintering methods

Jafar Baseri, Rahim Naghizadeh* and Hamid Reza Rezaie
School of Metallurgy and Materials Engineering, Iran University of Science and Technology, Narmak, Tehran, Iran

Alumina-spinel($NiAl_2O_4$, $CoAl_2O_4$ solid solution)-metal(nickel, cobalt solid solution) composites were fabricated by partial reduction of spinel in carbon-bed and sintered with three different processes namely, pressureless, hot pressing, and spark plasma sintering (SPS). The microstructural features and mechanical properties of composites were investigated. The pressureless samples, SPS samples, and hot pressed samples reached > 91%, > 97% and > 98% theoretical density, respectively. The flexural strength of SPS, hot pressed, and pressureless samples were about 415 MPa, 367 MPa, and 247 MPa, respectively. Vickers Microhardness of SPS, hot pressed, and pressureless sintering were about 15.3, 14.5, and 10.98 GPa, respectively. The fracture toughness of SPS and hot pressed samples did not have a significant difference, and they were about 7.2 and 7.8 MPa.$m^{1/2}$, repectively.

Key words: Alumina (Al_2O_3), Composite, Nickel, Cobalt, Pressureless, Spark plasma sintering (SPS), Hot Press, Mechanical properties.

Introduction

Alumina is one of the most common ceramics which is used in industries such as electrical insulators, cutting tools, refractories, to name but a few. This is because of its wonderful thermal stability, hardness, and refractoriness properties. However, relatively low fracture toughness and strength of ceramics limit its engineering application. Nowadays, many researchers have focused on improving the mechanical properties of ceramics in general and alumina in particular with secondary phases. They have reinforced ceramics with both metal and ceramic particles [1-4].

Some studies were done on alumina-zirconia composites [5-7], alumina-SiC composites [8-10] and many other alumina-ceramic composites. In addition to this, some studies have focused on alumina-metal composites such as alumina-copper composites [11-14], alumina-silver composites [15-16], alumina-tungsten composites [17], alumina-iron composites [18], alumina-molybdenum composites [19], alumina-chromium composites [20-22], alumina-cobalt composites [23], and alumina-nickel composites [1-4], however alumina-metal solid solution is comparatively less investigated.

Three main sintering techniques of ceramic powders are pressureless, hot pressing [8, 11, 25], and spark plasma sintering [26-27]. Pressureless is the cheapest and most available sintering method, but obtaining full density or a density close to the theoretical density is very difficult by using this method [3]. The next sintering method is hot pressing. This method can provide a high relative density and defect-free sample. But this method, due to its time-consuming densification process, cannot provide a fine microstructure in compare to SPS method.

In spark plasma sintering (SPS) or pulsed electric current sintering (PECS), a high pulsed electric current is provided to carry out high-speed sintering of the powder. These high pulsed electric currents cause a heating rate of 1000 K/min. So by this technique, a fine microstructure, and high relative density can be reached simultaneously [26-27].

Due to the less investigation have done on the alumina-metal solid solution and alumina-spinel especially on their mechanical properties, in this study, a batch consists of Al_2O_3, Ni, Co, $NiAl_2O_4$, and $CoAl_2O_4$ was provided. With considering that Ni and Co are entirely soluble in each other and, also $NiAl_2O_4$ and $CoAl_2O_4$ are soluble in each other too, therefore, a three-phase composite (Alumina, Ni-Co solid solution, Al_2O_4-$NiAl_2O_4$ solid solution) was provided. Sintering of this batch was investigated in three ways, namely, pressureless, hot press, and SPS.

Experimental

Preparation of composites

Reactive alumina powder (PFR20, Alteo, France), nickel sulfate powder (99% purity, China), and cobalt sulfate powder (99% purity, China) were mixed and then ball milled in a polyethylene container using alumina milling balls and high purity methanol for 4 hours. The amount of nickel sulfate and cobalt sulfate were

*Corresponding author:
Tel : +982177240291
Fax: +982177240291
E-mail: rnaghizadeh@iust.ac.ir

controlled to result in 5 Vol% Ni and 5 Vol% Co in the composite after a complete reduction. The methanol was then removed by drying on a hot plate. The dried samples were crushed and passed through a 60 mesh sieve. Thermogravimetry (TG) and differential thermal analysis (DTA) analysis of the precursors were performed by using a DTA/TGA analyzer (STA 504, Bähr, Germany) in air atmosphere with a heating rate of 10 K/min. The precursors were calcined in air atmosphere at 1000 °C for 3 hours to achieve $NiAl_2O_4$, $CoAl_2O_4$, and Al_2O_3 without any residual NiO nor CoO. The powder was then partially reduced in carbon-bed at 1420 °C for 12 hrs. In this stage, alumina, $NiAl_2O_4$, $CoAl_2O_4$, Ni, and Co existed in this batch. The reduced powder was ball milled again for 4 hrs to break the agglomerates. Finally, the powder was dried on a hot plate and then sieved.

For pressureless sintering, powder compacts were formed by uniaxially pressing at 18 MPa (the mold diameter was 50 mm), and then by cold isostatic pressing (CIP) at 400 MPa. Pressureless sintering was done under carbon-bed atmosphere at 1600 °C for 4 hrs.

For hot press sintering, FAST method (field assisted sintering technique/direct hot pressing) was used. The powder was loaded into a 50 mm diameter graphite die and was then pressed at 30 MPa and heated at 1380 °C for 30 minutes.

For SPS, the powder was loaded into a 50 mm diameter graphite die and was then pressed at 30 MPa and heated at 1380 °C for 10 minutes.

Characterization

The relative density of the samples was measured by the Archimedes method using water. The sintered bodies were cut by a micro cutter with a diamond blade, then ground and polished with diamond paste to obtain mirror surfaces. The final dimensions of these samples were $3.5 \times 3.5 \times 45$ for bending strength test. The fracture strength of the samples was measured by a 3-point bending test with a span length of 16 mm and a crosshead speed of 0.5 mm/min (DBBP-500, Bongshin, Korea). The microstructural and energy-dispersive X-ray spectroscopy (EDS) analysis of the polished samples were investigated by scanning electron microscopy (SEM, Tescan, VEGA//XMU). The X-ray diffraction patterns of the samples were accomplished by a (X'PERT PRO; Philips, Eindhoven, The Netherlands) diffractometer using a Cu-target tube ($\lambda = 0.15$ nm). The patterns were recorded in the $2\theta = 10°$-$80°$ range at room temperature, with a scanning rate of $0.001° \ S^{-1}$ and a step interval of 0.02°. The Vickers microhardness (H_v) of the sintered composites was measured on polished surfaces with a load of 10 kg using Vickers hardness tester (V-test II, Bareiss). Fracture toughness (K_{IC}) was evaluated by direct crack measurement method with a load of 10 kg and a crosshead speed of 100 μm/sec in the same apparatus, using Evans and Charles formula [28, 29].

Results and Discussion

Calcination

The TG/DTA curves of the powder are shown in Fig. 1. The endothermic peak at 151 °C is related to the partial dehydration of sulfates, accompanied by a significant weight loss.

$$NiSO_4 \cdot 6H_2O \rightarrow NiSO_4 \cdot H_2O + 5H_2O \quad [31]$$
$$CoSO_4 \cdot 6H_2O \rightarrow CoSO_4 \cdot H_2O + 5H_2O \quad [30]$$

The second endothermic peak at 351 °C is related to the last stage of dehydration of sulfates, accompanied by a weight loss.

$$NiSO_4 \cdot H_2O \rightarrow NiSO_4 + H_2O \quad [31]$$
$$CoSO_4 \cdot H_2O \rightarrow CoSO_4 + H_2O \quad [30]$$

The last endothermic peak at 846 °C is due to the decomposition of sulfates and the crystallization of the $CoAl_2O_4$ and $NiAl_2O_4$ spinel, accompanied by a significant weight loss. These reactions are composed of decomposition of sulfates with a considerable positive enthalpy and crystallization of spinels with a negative enthalpy. Considering these, the total enthalpy is positive. So the related pick is endothermic [30-32]. There is no significant weight loss at higher temperatures.

$$NiSO_4 + Al_2O_3 \rightarrow NiAl_2O_4 + SO_3 \quad [31]$$
$$CoSO_4 + Al_2O_3 \rightarrow CoAl_2O_4 + SO_3 \quad [30]$$

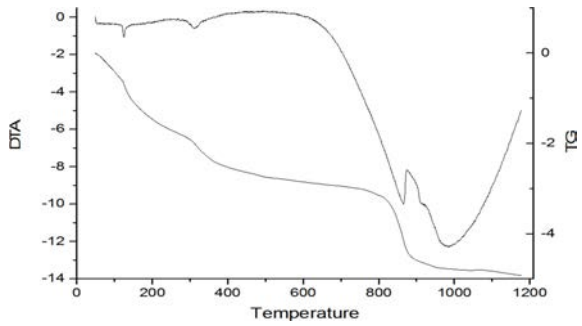

Fig. 1. DTA-TG pattern of raw material in air atmosphere with heating rate of 10 K/min.

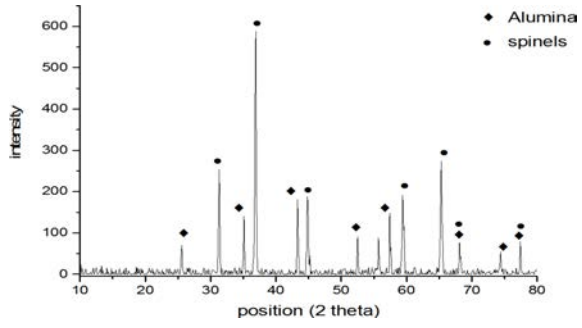

Fig. 2. XRD pattern of calcined powders at 1000 °C for 3 hrs.

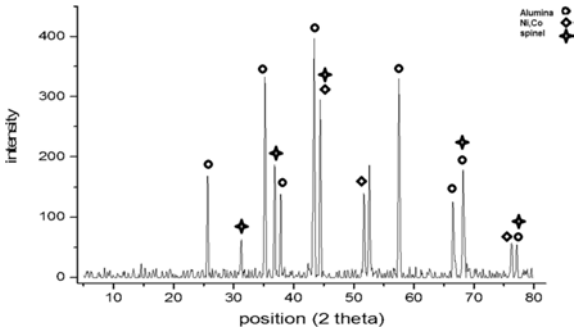

Fig. 3. XRD pattern of partially reduced powders at 1420 ºC for 12 hrs at carbon-bed.

Fig. 2 shows the X-ray diffraction pttern (XRD) of calcined powder at 1000 ºC for 3 hrs. The peaks are related to alumina and spinels and no other oxide phase was detected.

Reduction

Partially reduction of calcined powders happened at 1420 ºC for 12 hours. The carbon existed in carbon-bed could burn efficiently in lack of oxygen and produce CO gas. This gas could partially reduce spinels:

$$NiAl_2O_4 + CO_{(g)} \rightarrow Ni + Al_2O_3 + CO_2 \quad [35]$$

$$CoAl_2O_4 + CO_{(g} \rightarrow Co + Al_2O_3 + CO_2 \quad [36]$$

Fig. 3 shows the X-ray diffraction pattern of the partially reduced powder. It could be clearly observed that NiO and CoO peaks were not detected. As the figure shows, alumina, Ni-Co solid solution and also spinel solid solution ($NiAl_2O_4$-$CoAl_2O_4$) were detected.

Microstructure

Fig. 4 shows the microstructure of (a) SPS, (b) hot press, and (c) pressureless samples. In SPS samples,

Table 1. EDS results.

		SPS	Hot press	Pressureless
White phase	Al	5	7	8
	Ni	43	44	44
	Co	52	49	48
Bright gray phase	Al	63	60	–
	Ni	21	23	–
	Co	16	17	–
Dark gray phase	Al	94	93	90
	Ni	3	3	6
	Co	3	4	4

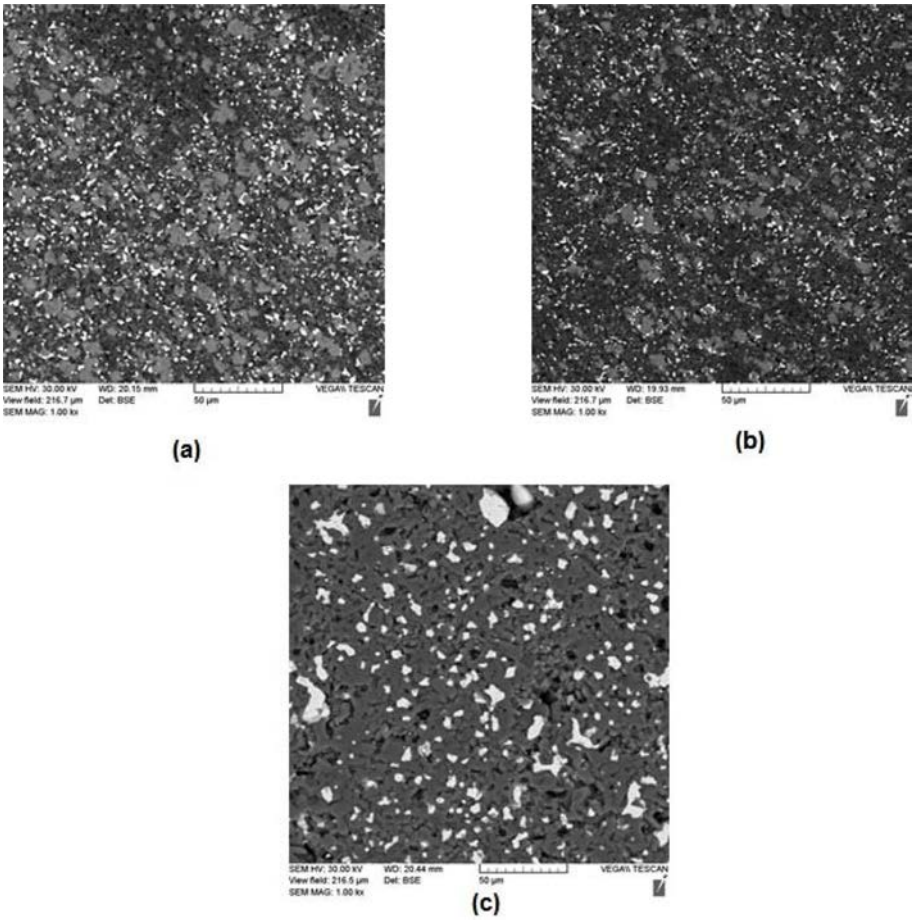

Fig. 4. Microstructures of (a) SPS, (b) hot press, and (c) pressureless samples.

Table 2. Phase vol% of samples calculated by image analyzer software (Celemex).

	Metal	Spinel	Alumina
SPS	5.1	28.3	66.6
Hot pressing	7.5	15.3	77.2
Pressurelss sintering	9.8	0	90.2

there are three phases according to the back scatter contrast. Based on EDS analysis (Table 1) the white phase is Ni-Co solid solution; the light gray phase is a solid solution of $NiAl_2O_4$ and $CoAl_2O_4$; and the dark gray phase is alumina. The spinel phase in SPS samples is more often than hot pressed samples. As Table 2 shows, SPS samples have 5% metal phase and 15% spinel phase, while hot pressed samples have 8% metal phase and 9% spinel. This may be because the sintering action was done in a vacuum inside a carbon die for both methods. The carbon die can spread some CO gasses. This gas can lead spinel to reduce to metal and alumina. As to the more time that hot press process

Table 3. Relative densities of samples.

Samples	Hot press	SPS	Pressureless
Relative density	98.2%	97.5%	91.2%

samples need to sinter, the spinel phase in hot pressed samples has been more reduced than the spinel phase in SPS samples. Jinsu et al. proved this phenomenon in their works [28]. The spinel phases in pressureless samples were reduced completely, due to enough sintering time discussed above.

Due to the rapid sintering of SPS samples, the average grain size of these samples was smaller than the average grain size of hot pressed samples and pressureless sintered samples.

Fig. 5 shows the fracture surface of (a) SPS, (b) hot pressed, and (c) pressureless sintered samples. In these SEM images, many voids are visible. In pressureless samples, many of these voids were related to low relative density (relative density of samples is shown in Table 3) while the voids in SPS and hot pressed

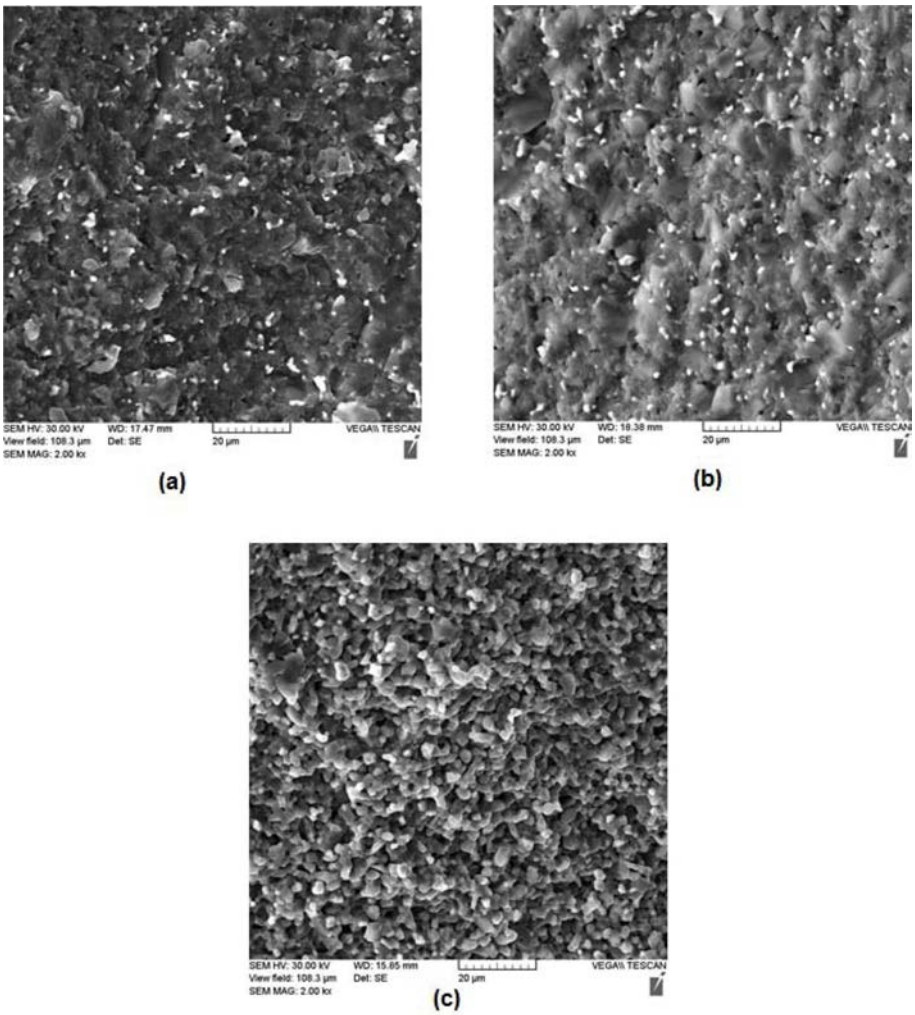

Fig. 5. Fracture surfaces of (a) SPS, (b) hot pressed, and (c) pressureless sintered samples.

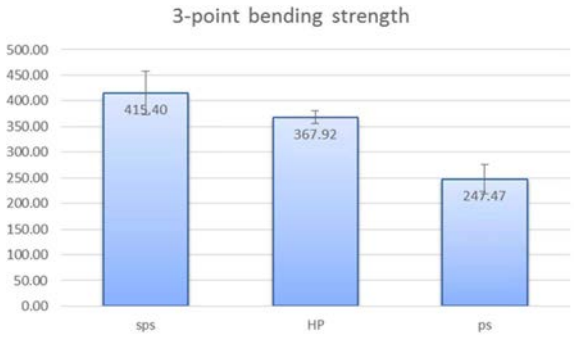

Fig. 6. 3-point bending strengths of samples.

Table 4. Mechanical properties of samples.

	SPS	Hot press	Pressureless
3-point bending strength	415.4 ± 32.8	367.9 ± 11.8	247.5 ± 28.8
Micro-hardness (GPa)	15.3 ± 0.2	14.5 ± 0.4	10.98 0.06
Toughness (MPa.m$^{0.5}$)	7.2 ± 0.5	7.8 ± 0.3	–

samples and some voids in the pressureless samples were formed by metal grain peeling of spinel and alumina matrix. This phenomenon affects fracture of ceramics and results in improvement of fracture strength as well as the fracture toughness.

Mechanical properties

Table 3 shows the relative density of samples. The relative density of pressureless samples is significantly lower than the other two methods. In hot pressing and spark plasma sintering, the applied pressure during the sintering period has a considerable influence on densification. The difference between related densities of mentioned methods is negligible.

Fig. 6 shows 3-point bending strengths of samples that calculated from the following equation:

$$\sigma = \frac{3Pl}{2b^2 d} \quad (1)$$

where P is the applied load, l is support spans distance, b is the depth of test beam, and d is the width of test beam [29].

The bending strengths of these samples are increased with decreasing the grain size of samples. As to the absence of applied pressure during the sintering, pressureless samples have the least strength, although the metal phases in pressureless samples, which increases the strength, are more often than other samples Also, the time-consuming process of this method leads to exponentially growing of the grain size.

Table 4 shows the microhardness of samples. The average microhardness was acquired from 10 indentations for each sample. As this table shows, the SPS samples have the highest hardness which is due to the small grain size of SPS samples. Also in hot pressed samples, because of the more reduction, there are more ductile phases which decrease the micro-hardness. In addition to that, in hot pressed samples, the grain size of ductile phases is larger than SPS samples.

Table 4 also shows fracture toughness of samples which evaluated by this formula [28-29]:

$$where \frac{c}{a} \geq 2.5 \quad K_{Ic} = \frac{0.129\left(\frac{c}{a}\right)^{-\frac{3}{2}}}{\left(\frac{\varphi}{Ha^{\frac{1}{2}}}\right)\left(\frac{H}{E.\varphi}\right)^{\frac{2}{5}}} \quad (2)$$

where K_{Ic} is fracture toughness, c is half length of the crack generated by indentation, a is half length of the indentation diagonal, φ is a constant, H is Vickers hardness, and E is the modulus of elasticity. According to statistical analysis, there are no significant differences between the fracture toughness of SPS and hot pressed samples [30]. In this study, the fracture toughness of pressureless samples could not be determined due to the presence of more voids in comparison to other samples, which prevent crack growth by blocking them.

Summary

In this paper, a three-phase cermet composite (Al_2O_3; $NiAl_2O_4$-$CoAl_2O_4$ solid solution; Ni-Co solid solution) was prepared and sintered with three different techniques namely, SPS, hot press, and pressureless methods. The mechanical properties of pressureless samples were not as well as the other two methods. The hot pressed samples had the most relative density, while micro-hardness and bending strength of SPS samples were better than the other samples. In this study, no significant difference between fracture toughness of the SPS and the hot press was observed. Also, the fracture toughness of pressureless samples by indentation method could not be measured. The authors suggest for further studies; researchers can use other methods like Single Edged Notch Beam test [29] to evaluate fracture toughness of bodies with < 95% of theoretical density.

References

1. K. Konopka, L. Lityńska-Dobrzyńska, and J. Dutkiewicz, Solid State Phenom.186 (2012) 222-225.
2. I. liberthal, Micheal, W.D. Kaplan, Mater. Sci. Eng. A302 (2001) 83-91.
3. R.Z. Chen and W.H. Tuan, J. Eur. Ceram. Soc. 19 (1999) 463-468.
4. N.L. Barham, W.D. Kaplan, and D. Rittel, Mater. Sci. Eng. A597 (2013) 1-9.
5. H.L.C. Pulgarin and M.P. Albano, Mater. Sci. Eng. A639 (2015) 136-144.

6. R. Benavente, M.D. Salvador, F.L. Penaranda-Foix, E. Pallone, and A. Borrell, Ceram. Int. 40[7] (2014) 11291-11297.
7. A. Rittidech and N. Suekwamsue, Ceram. Int. 41 (2015) S123-S126.
8. M. Parchovianský, D. Galusek, J. Sedláček, P. Švančárek, M. Kašiarová, J. Dusza, and P. Šajgalík, J. Eur. Ceram. Soc. 33[12] (2013) 2291-2298.
9. D.-Y. Lee and D.-H. Yoon, Ceram. Int. 40[9] (2014) 14375-14383.
10. L. Carroll, M. Sternitzke, and B. Derby, Acta Mater. 44[11] (1996) 4543-4552.
11. L. Wang, J.-L. Shi, M.-T. Lin, H.-R. Chen, and D.-S. Yan, Mater. Res. Bull. 36[5-6] (2001) 925-932.
12. Q.B. Nguyen, K.S. Tun, C.Y. H. Lim, W.L.E. Wong, and M. Gupta, Compos. B Eng. 55 (2013) 486-491.
13. S.T. Oh, T. Sekino, and K. Niihara, J. Eur. Ceram. Soc. 18[1] (1998) 31-37.
14. K. Jach, K. Pietrzak, and A. Wajler, Powder Metallurgy and Metal Ceramics 52[11] (2014) 680-685.
15. A.K. Dutta, J. Mater. Sci. Lett. 20 (2001) 917-919.
16. A.K. Dutta, N. Narasaiah, A.B. Chattopadhyaya, and K.K. Ray, Ceram. Int. 27 (2001) 407-413.
17. T. Sekino and K. Niihara, Nano Structured Mater. 6 (1995) 663-666.
18. P.A. Trusty and J.A. Yeomans, J. Eur. Ceram. Soc. 17[4] (1997) 495-504.
19. K. Konopka, M.S. Maj, and K.J. Kurzydłowski, Mater. Charact. 51[5] (2003) 335-340.
20. Y. Ji and J. Yeomans, J. Eur. Ceram. Soc. 22 (2002) 1927-1936.
21. K. Pietrzak, M. Chmielewski, and W. Wlonsinski, Sci. Sinter. 36 (2004) 171-177.
22. C. Marcin and P. Katarzyna, J. Eur. Ceram. Soc. 27 (2007) 1273-1279.
23. B.T. Lee, K.H. Kim, H.M.E. Rahman, and H.Y. Song, Mater. Trans. 49[6] (2008) 1451-1455.
24. N. Travitzky and A. Shlayen, Mater. Sci. Eng. A 244[2] (1998) 154-160.
25. A. Mocellin, E. Mines, P. De Saurupt, and N. Cedex, J. Eur. Ceram. Soc. 18 (1998) 1743-1752.
26. M. Suárez, A. Fernández, J.L. Menéndez, R. Torrecillas, H.U. Kessel, J. Hennicke, R. Kirchner, and T. Kessel, in Sintering Application (2013) 319-324.
27. M. Demuynck, J.P. Erauw, O. Van der Biest, F. Delannay, and F. Cambier, J. Eur. Ceram. Soc. 32[9] (2012) 1957-1964.
28. A.G. Evans and E.A. Charles, J. Am. Ceram. Soc. 59[7-8] (1976) 371-372.
29. J.B. Wachtman, W.R. Cannon, and M.J. Matthewson, Mechanical Properties of Ceramics (2009).
30. J. Donaldson and D. Beyersmann, "cobalt and cobalt's compound," in Ullmann's Encyclopedia of Industrial Chemistry, Weliy, 2005.
31. J. Straszko, J. Mozejko, and M. Olszak-humienik, J. Therm. Anal. 45 (1995) 1109-1116..
32. K. Lascelles, L.G. Morgan, D. Nicholls, and D. Beyersmann, "nickel," in Ullmann's Encyclopedia of Industrial Chemistry, 2005.
33. J.S. Lu, L. Gao, J. Sun, L.H. Gui, and J.K. Guo, Mater. Sci. Eng. A 293[1-2] (2000) 223-228.
34. J.R. Taylor, An Introduction to Error Analysis: The Study of Uncertainties in Physical Measurements, University Science Books, 1997.
35. J.H. Krasuk, and J.M. Smith, AIChE J. 18 (1972) 506-512. doi:10.1002/aic.690180308.
36. S. Guo, S. Zhang, L. Wu, and S. Sun, Angew. Chem. Int. Ed. 51 (2012) 11770-11773. doi:10.1002/anie.201206152.